

Measurement of the magnetic and thermal characteristics of ferrites for a 300 kHz AC dipole for the Mu2e experiment

G. V. Velev, D. J. Harding, I. Iedemska, V. S. Kashikhin, V. V. Kashikhin, A. Makarov, A. Makulski, D. Orris

Abstract—A charged lepton flavor violation experiment, Mu2e, is planned at Fermilab, searching for muon to electron conversions with an unprecedented sensitivity, better than 6×10^{-17} at 90% CL. To achieve such sensitivity the incoming beam must be highly suppressed during the window for detecting the muon decays. One proposal for beam extinction is based on a collimator with two dipoles running in a resonant circuit at ~ 300 kHz synchronized to the bunch spacing. An appropriate choice of the ferrite material for the magnet yoke is critical to ensuring the reliable operation of such a high frequency dipole over the life of the experiment. In this paper, we present the results of the thermal and magnetic measurements of the selected ferrite material, including the field non-linearity effects and power losses. Some dimensional optimization of the ferrite bricks is also discussed.

Index Terms—Accelerator magnets, Ferrites, Magnetic measurements

I. INTRODUCTION

AFTER the completion of the Tevatron collider run in 2011 several new experiments are proposed for Fermilab's physics program. One of these experiments is the so-called Mu2e, which is planned to start operation in the next decade. It will provide the capability to search for charged lepton flavor violation with an unprecedented sensitivity of 6×10^{-17} at a 90% confidence level. Such sensitivity is approximately four orders of magnitude better than the current limits.

The Mu2e experimental technique can be found elsewhere [1] (see Chapter II). An important part of this technique is a specially structured 8 GeV proton beam that consists of short (~ 100 ns) bunches and relatively long gaps between the bunches of approximately $1.7 \mu\text{s}$ (Fig.1). Within these long gaps, the muons produced in the forward target and captured in the secondary target can be converted to electrons, if the e - μ lepton flavor is non-conserved. In practice, this means that the Mu2e detector will be triggered to record events during these beam gaps. To suppress any unwanted events,

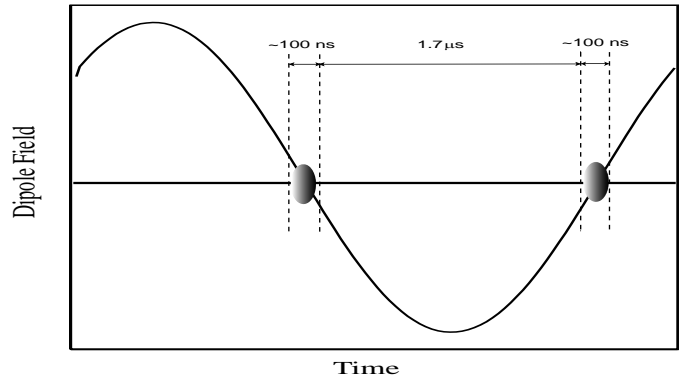


Fig. 1. A concept how the AC dipole should work to clean the protons between bunches. The beam is transmitted when the sine wave is approaching the zero crossing.

which may occur during the muon transport to and capture in the secondary target, it is crucial that protons are extinguished at the level of 10^{-9} during these intervals between bunches.

To achieve such unprecedented proton-free gaps at least two suppression methods should be applied. The first method is a passive one and relies on the bunch generation prescription (see Section 6 of ref. [1]). The second method, an active one, is based on the implementation of relatively high magnetic field AC dipole magnets. This paper describes the magnetic and thermal measurements of the ferrite samples considered for these magnets, as well as some optimization of the magnet design and ferrite sizes.

II. MAGNET SPECIFICATIONS

The technique of using AC dipoles for cleaning the beam gap is described in detail elsewhere [2]. The main idea is to utilize two AC dipoles separated by a beam collimator. Both dipoles are driven by sine amplitude waves, which are shifted by 180 degrees in phase with a frequency of approximately 300 kHz ($((1/1.7 \cdot 10^{-6})/2 \approx 600 \text{ kHz})/2 \approx 300 \text{ kHz}$). The factor of two comes from the fact that the beam is transported on the nodes when the sinus amplitude is approximately zero (Fig. 1). The second magnet cancels any bunch deviation caused by the first one.

The required aperture of the magnet is $5 \times 1 \text{ cm}^2$, which is wider in the plane where the beam is bent. The peak magnetic field is determined by the beam extension channel geometry with an optimal value of 0.06 T for a magnet length of 2 m.

Two of the proposed magnet cross-sections are shown in

Manuscript received 19 October 2009. This work was supported by the U.S. Department of Energy.

D. J. Harding, V. S. Kashikhin, V. V. Kashikhin, A. Makarov, A. Makulski, D. Orris, G. V. Velev are with Fermilab, P.O. Box 500, Batavia, IL 60510, USA, (e-mail: velev@fnal.gov).

I. Iedemska is with Moscow Institute of Physics and Technology, Moscow, Russia.

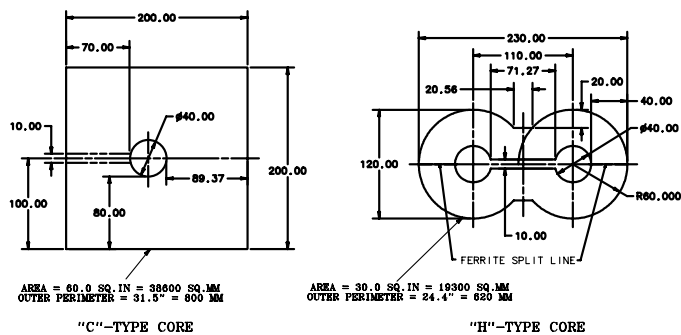


Fig. 2. The proposed cross-sections for the AC dipole.

Fig 2. The first one, called a C-shape type magnet (Fig.2 left), has a similar structure to a transmission line magnet (for example see Ref. [3]). The proposed drive conductor is a Litz cable with a diameter of 25 mm. This cable is epoxied to a ceramic tube, which is placed in the central hole of the ferrites. Additionally, a copper heat exchanger tube, used for the circulation of cooling water, is located inside the ceramic.

For the second cross-section type, an H-type magnet, the conductor is a simple copper pipe passing through the ferrite holes. For this design the cooling channels are attached to the outside surface of the ferrite. The advantage of this geometry is better heat dissipation, however, the disadvantage is the complex ferrite geometry, which drives up the price of the AC dipole.

The magnet will be placed in a vacuum box and the proton beam will pass directly through the magnet aperture. This requirement comes from the impracticality to produce long, more than 2 m, ceramic beam chambers with relatively thin walls ~ 1 -2 mm. Due to an expected large heat load from the eddy currents no metal beam chambers are being considered.

III. FERRITE SELECTION

The main issue in the design of a 300 kHz dipole magnet is the ferrite material losses and consequently the ferrite overheating. The problem is even more complicated because the magnet should continuously work in vacuum.

The ferrite material was pre-selected based on a 3D magnetic field transient analysis simulated with OPERA [4] and ferrite parameters presented in different publications [5].

Two classes of ferrites were considered: NiZn and MnZn. The main advantage of the NiZn ferrite is a very high volumetric resistivity. In this case, there is no need for high voltage insulation between the drive conductor and the ferrite plates. The drawback of this material is a high hysteresis loss, which is on the order of 2.5 W/cm^3 at 300 kHz (measurements by Walker Scientific Inc. [6]).

The MnZn type ferrites have about a factor of two lower losses at the same magnetic field and frequency. Several types of MnZn ferrites were tested by outside vendors – the results are summarized in the Table 1. The first three samples were measured by Walker Scientific Inc. and the other three by JC Sun [7].

The ferrite material MN60LL was chosen as a promising option due to its low losses and modest coercive force; the later parameter primarily defines the hysteresis loss. Moreover, for the MN60LL ferrite there is a large dependence

TABLE I. FERRITE TEST RESULTS AT 300 kHz

MnZn ferrites	Ferrite losses (W/cm^3)	B_s (T)	H_c (A/m)
MN80C	1.0	0.49	14.3
MN8CX	0.46	0.45	15.9
M100	0.96	0.45	2.4
M25	0.98	0.41	4.8
MN60	0.87	0.45	6.4
MN60LL	0.52	0.45	6.4

of the hysteresis loss on the temperature due to a substantial change of the relative permeability. For example, the hysteresis loss could increase by a factor of 3 when the temperature of the ferrite core changes from 20° to 100° C.

In order to reduce the project risk, optimize the ferrite geometry, and test the cooling alternatives, measurements of three MN60LL plates with the proposed C-type magnet design geometry were carried out.

IV. MEASUREMENT SETUP

The schematic of the measurement setup is shown in Fig. 3. The ferrite sample is mounted in an aluminum box, which serves as Faraday cage for the experiment. The internal walls of the box are covered with thermo-insulation foam to prevent the heat convection between the ferrite and the aluminum walls. Thus, we try to simulate an operation similar to the beam condition where ferrites will be used in the vacuum.

The test samples are C-type ferrite plates, shown in Fig.2 left, without the beam gap. The sample has a box shape with dimensions of $200 \text{ mm} \times 200 \text{ mm} \times 10 \text{ mm}$. The diameter of

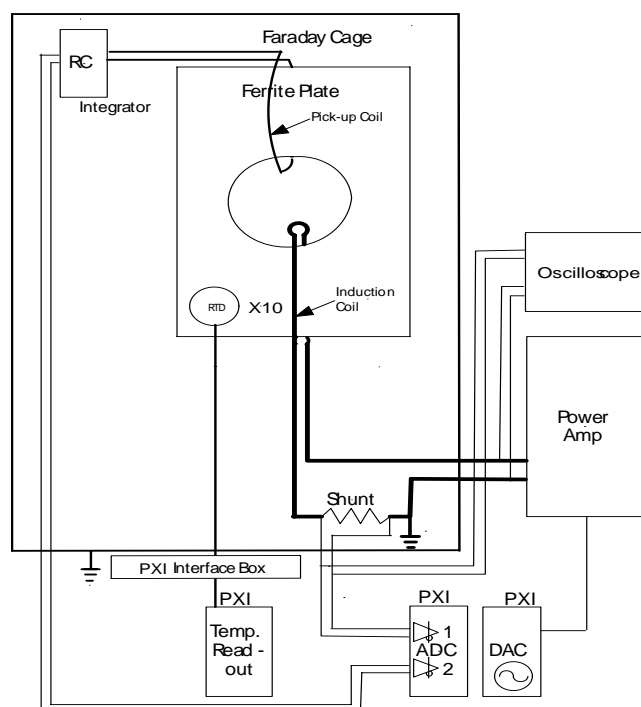


Fig. 3. Schematic of the ferrite test system.

the conductor hole is 40 mm and the center of the hole is offset by 10 mm from the center of the square. To cool the sample, a cooling channel fabricated from copper tube was glued around of the three sides of the ferrite perimeter. Two aluminum plates were glued to the top and bottom sides to help with the additional heat dissipation. On average, the cooling water temperature and pressure were approximately 21 C and 30 psi when testing.

The data acquisition system is based on the following National Instruments (NI) DAQ modules (Fig. 3) [8]. A PXI-5402, 20 MHz arbitrary function generator is used to provide the 300 kHz driving signal to the NIE power amplifier, which provides the current for the excitation coil. A PXI-5122, 14 bit 100MHz analog-to-digital converter, is used to digitize the voltages proportional to the current and field flux density from the pick-up coil; and a PXI-4351 precision temperature logger, which is used to measure the temperatures of 10 resistance temperature detectors (RTDs), placed on the surface of the sample.

A fast 2 GHz LeCroy (model 204 MXi) oscilloscope was used to measure the power total losses in the ferrite. This was carried out by detecting simultaneously the input voltage and the current from the power amplifier. A correction for the losses in the shunt and the excitation coil was then applied.

V. DATA ANALYSIS AND COMPARISON TO THE MODEL

The BH curves for typical measurements at different frequencies are shown in Fig. 4. To calculate the magnetic field strength (H), the measured current is normalized to the effective length of the flux lines. The average magnetic flux density (B) is derived by dividing the magnet flux, which is proportional to the voltage from the RC integrator, by the effective area. This area is calculated in the toroidal approximation with the internal and external radii of 20 mm and 90 mm correspondingly. The first number corresponds to the radius of the conductor hole (Fig. 2) and the second one is the distance from the center of the hole to the closest edge of the ferrite plate.

The total AC losses in the ferrite plates are proportional to the area inside B-H curve. A quantitative conclusion from the B-H measurements, driven by the rapid increase of the area

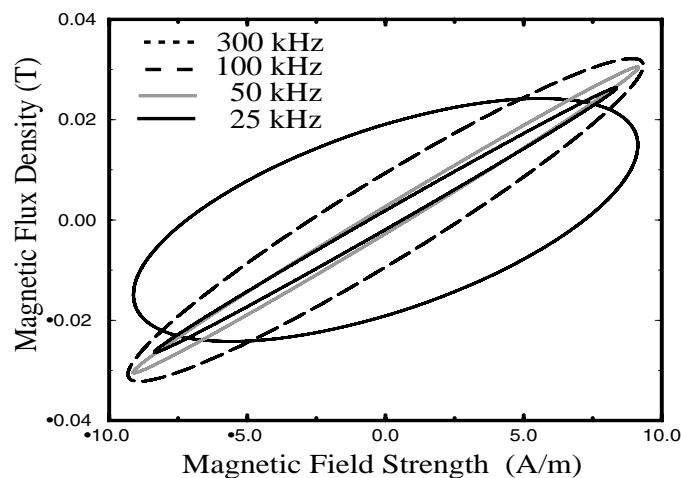


Fig. 4. B-H curves versus frequency at current of 2.3 A

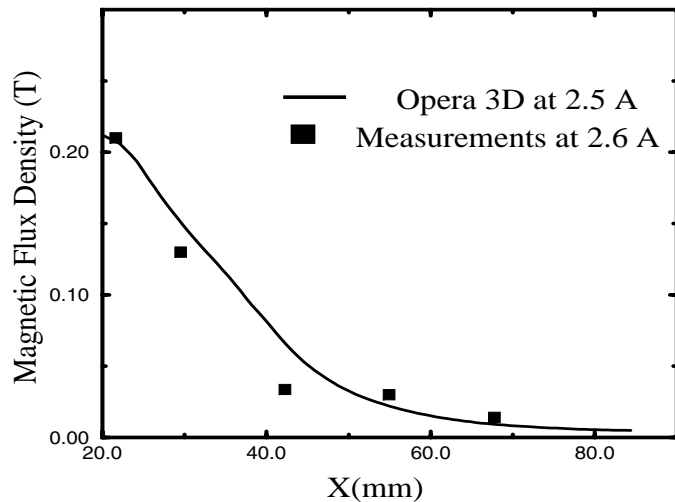


Fig. 5. Flux density distribution along the ferrite plate. The solid line is the result from OPERA calculations, the squares are result from a measurement.

with the frequency, is that the ferrite performance is limited by the eddy current loss, while the hysteresis loss is relatively small (for example, the area of the 25 kHz B-H curve gives a first order estimation for the effect from the hysteresis loss).

For an excitation frequency of 300 kHz and using the MN60LL ferrite material, a factor of two discrepancy was observed between the flux density values B obtained in our measurements and the results presented in Table 1. This discrepancy can be explained by the different geometry of the ferrite samples. The measurements associated with Table I were made of ferrite toroids with small differences between the internal diameter (ID) and external diameter (OD) (ID = 41.1, OD = 50.0 and height = 13.0 mm). However, in our case, the ferrite thickness (difference between OD and ID) is 70 mm, which makes the flux density distribution very uneven. For example, one could expect a strong field around the conductor hole, which rapidly decreases with increasing distance from the center.

To confirm this hypothesis, a simulation using OPERA was performed (Fig. 5, solid curve). In addition, a test was carried out using one of the ferrite samples in which small holes were drilled along the ferrite plate in the region of interest. Using these holes, partial loops were formed and we measured the differential flux density. The result is compared with the simulation (Fig. 5, squares) and a good agreement is observed. An important conclusion from this comparison is that in the case of the C-shape cross-section, the ferrite thickness might be reduced from 70 to 50 mm without significantly decreasing of flux density B.

During the measurements, the ferrite temperature was monitored by 10 RTDs. They were glued on the surface of the ferrite samples in the following positions: four of them were placed around the conductor hole every 90 degrees, four more were placed in a vertical direction to the ferrite edge with cooling, and two more in the horizontal direction to the ferrite edge without cooling.

As expected, the fastest temperature rise was detected in the RTD placed closest to the conductor hole in the quadrant not covered by a cooling channel. Fig. 6 shows the temperature change in this quadrant versus time for different amplitudes of

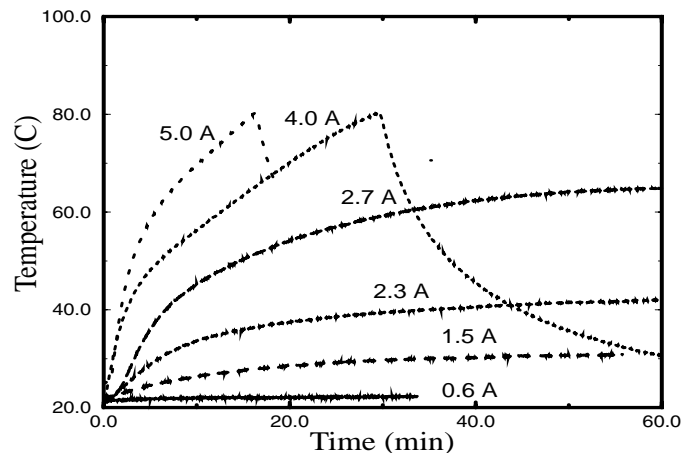


Fig. 6. The highest temperature detected by the RTDs versus current amplitude.

the excitation current. In order to protect the ferrite from overheating around the conductor hole, where the maximum concentration of the magnetic flux is found, the current was switched off if any of the RDTs detected temperature greater than 80°C . From the time-temperature dependence, one can conclude that the maximum operation current for a ferrite with such dimensions and cooling scheme is around 2.3-2.7 A.

Additional information contributing to the determination of the operational current limits is the dependence of the relative ferrite permeability on the temperature. This effect is shown in Fig. 7 where the ferrite temperature and flux density are plotted versus time for a current amplitude of 2.7 A. At the beginning of the measurement, when the ferrite sample is still at room temperature, the average flux density is 0.037T. After 50 minutes, the temperature of the ferrite sample increases to 63°C and B decreases to 0.023 T. This field can be obtained with 16% lower current (2.3 A) and less heat dissipation.

Table II summarizes the results from performed measurements at different currents. The starting temperature for all measurements was 21°C . In the case of the last two measurements at 4 A and 5 A, the temperatures did not reach a plateau so they were terminated at 80°C . The maximum flux density of 0.024 T and stable temperature (42.4°C) of the ferrite sample was measured at a current amplitude of 2.3 A. One may conclude that the preferred operational current for the proposed cooling scheme will be in the region of 2.3 A.

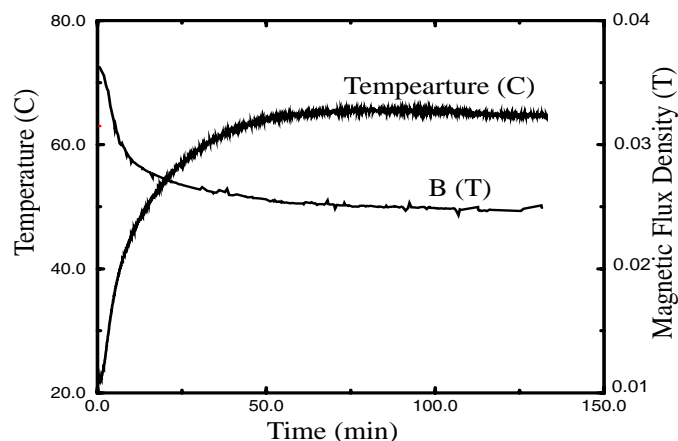


Fig. 7. The temperature and flux density dependence versus time at 2.7 A.

TABLE II. FERRITE TEST RESULTS AT DIFFERENT CURRENTS

Current (A)	B at the start (T)	B at the end (T)	Maximum T the end (C)
0.6	0.007	0.007	22.3
1.5	0.016	0.019	30.9
2.3	0.030	0.240	42.4
2.7	0.034	0.230	64.3
4.0	0.057	0.280	80.9*
5.0	0.673	0.290	80.8*

*The measurements did not reach a temperature plateau.

VI. SUMMARY

In this paper, we described measurements of the MN60LL ferrite material for 300 kHz AC dipoles. Two of these dipoles, which were designed as a transmission line magnets, are a major component of the proposed inter-bunch extinction scheme for the proton line of the future Mu2e experiment.

Using transmission line magnets in accelerator operations is a well-established technology; however, this is a first time such a powerful AC dipole with a high duty factor working in vacuum has been proposed.

As it was expected, the major problem for building such a dipole is to provide an adequate cooling of the ferrite plates. Moreover, we confirmed that the eddy current loss plays a major role in the heating.

We found that the initially proposed C-type plates cannot operate continuously with a field more than $B = 0.024\text{ T}$ although the requirement is 0.06 T for a 2 m long magnet. One of the possible solutions is to increase the length of the existing magnet design by a factor of 2.5; other possibilities include an optimization of the cooling scheme and ferrite shape.

If the ferrite cooling turns out to be impractical, a very different approach could be considered, which is dividing the AC dipole into several short sections and utilizing short ceramic beam chambers. In this case, the ferrite plates will be placed outside the beam vacuum and direct oil cooling is applicable.

REFERENCES

- [1] Mu2e Collaboration, "Proposal to search for $\mu\text{N} \rightarrow e\text{N}$ with a single event sensitivity below 10^{-16} ," FERMILAB-PROPOSAL-0973, Oct. 2008.
- [2] E. J. Prebys *et al.*, "AC dipole system for inter-bunch beam extinction in the Mu2e beam line," in *Proc. 2009 Part. Acc. Conf.*, paper TU6RFP033.
- [3] G.W. Foster *et al.*, "Conductor design for the VLHC transmission line magnet," in *Proc. 1999 Part. Acc. Conf.*, pp. 182-184.
- [4] Opera software package, <http://www.vectorfields.com>.
- [5] Information collected from web pages and catalogs of Ceramic Magnetics Inc. <http://www.cmi-ferrite.com>, National Magnetics Group <http://www.magneticsgroup.com>, and Hitachi Metals, Ltd., <http://www.hitachimetals.com>.
- [6] Walker Scientific Inc., <http://www.laboratorio.elettrofisico.com>.
- [7] J.C. Sun, "Testing report Bst-FL 0809_A," Fermilab report, unpublished.
- [8] More information about the NI boards can be found at the web page: <http://www.ni.com>.